Stem Cell Reports
Article

OPEN ACCESS

Chemical Cocktails Enable Hepatic Reprogramming of Mouse Fibroblasts with a Single Transcription Factor

Ren Guo,[1,3,7] Wei Tang,[2,7] Qianting Yuan,[1] Lijian Hui,[4] Xin Wang,[5,6] and Xin Xie[1,2,*]

[1]CAS Key Laboratory of Receptor Research, National Center for Drug Screening, Shanghai Institute of Materia Medica, Chinese Academy of Sciences, 189 Guo Shou Jing Road, Shanghai 201203, China
[2]Shanghai Key Laboratory of Signaling and Disease Research, Laboratory of Receptor-based Bio-medicine, School of Life Sciences and Technology, Tongji University, Shanghai 200092, China
[3]University of Chinese Academy of Sciences, No. 19A Yuquan Road, Beijing 100049, China
[4]Laboratory of Molecular Cell Biology, Institute of Biochemistry and Cell Biology, Shanghai Institutes for Biological Sciences, Chinese Academy for Sciences, 320 Yueyang Road, 200031 Shanghai, China
[5]Key Laboratory of National Education, Ministry for Mammalian Reproductive Biology and Biotechnology, Inner Mongolia University, Hohhot 010021, China
[6]Department of Laboratory Medicine and Pathology, Stem Cell Institute, University of Minnesota, Minneapolis, MN 55455, USA
[7]Co-first author
*Correspondence: xxie@simm.ac.cn
http://dx.doi.org/10.1016/j.stemcr.2017.06.013

SUMMARY

Liver or hepatocytes transplantation is limited by the availability of donor organs. Functional hepatocytes independent of the donor sources may have wide applications in regenerative medicine and the drug industry. Recent studies have demonstrated that chemical cocktails may induce reprogramming of fibroblasts into a range of functional somatic cells. Here, we show that mouse fibroblasts can be transdifferentiated into the hepatocyte-like cells (iHeps) using only one transcription factor (TF) (*Foxa1*, *Foxa2*, or *Foxa3*) plus a chemical cocktail. These iHeps show typical epithelial morphology, express multiple hepatocyte-specific genes, and acquire hepatocyte functions. Genetic lineage tracing confirms the fibroblast origin of these iHeps. More interestingly, these iHeps are expandable *in vitro* and can reconstitute the damaged hepatic tissues of the fumarylacetoacetate hydrolase-deficient ($Fah^{-/-}$) mice. Our study provides a strategy to generate functional hepatocyte-like cells by using a single TF plus a chemical cocktail and is one step closer to generate the full-chemical iHeps.

INTRODUCTION

Liver failure is a life-threatening illness and one of the most common causes of mortality (Touboul et al., 2010). Orthotopic liver transplantation is a well-established procedure for the treatment of end-stage liver failure, but the application is limited by the availability of suitable organs (Dutkowski et al., 2011). Hepatocyte transplantation is a promising alternative to whole-organ transplantation to support many forms of liver failure (Dolgikh, 2012; Kasai and Sawa, 2000). However, the source of hepatocytes is still limited to donor livers. So. to generate functional and clinically applicable hepatocytes independent of donor organs is of great therapeutic interest.

Embryonic stem cell (ESC)-derived hepatocyte-like cells have been useful for basic research and drug discovery (Murry and Keller, 2008). However, the use of ESC-derived hepatocyte-like cells faces ethical and possible immune rejection problems. The induced pluripotent stem cell (iPSC)-derived hepatocytes may bypass some of these problems, but the tumorigenic nature of pluripotent stem cells still limits their direct clinical application (Shiota and Yasui, 2012).

Cell transdifferentiation, i.e., direct reprogramming of one somatic cell type into another cell type without passing through the pluripotent state offers new ways of generating functional hepatocytes (Du et al., 2014; Huang et al., 2011, 2014; Sekiya and Suzuki, 2011; Yu et al., 2013). Direct reprogramming of mouse fibroblasts into hepatocytes has been achieved *in vitro* by overexpression of the transcription factors (TFs) *Hnf4α* plus *Foxa1, Foxa2,* or *Foxa3*, or by the combination of *Gata4, Hnf1α,* and *Foxa3*, and inactivation of $p19^{Arf}$ (Huang et al., 2011; Sekiya and Suzuki, 2011). In addition, *Hnf1β* and *Foxa3* have been found to be sufficient to reprogram mouse fibroblasts into hepatic stem cells, which could be further differentiated into both hepatocytes and cholangiocytes (Yu et al., 2013). More interestingly, *in vivo* expression of *Foxa3, Gata4, Hnf1α,* and *HNF4α* with adenovirus also enabled the generation of hepatocyte-like cells from myofibroblasts in fibrotic mouse livers (Song et al., 2016). Human induced hepatocytes (hiHeps) have also been generated from fibroblasts by lentiviral expression of *Foxa3, Hnf1α,* and *Hnf4α* (Huang et al., 2014), or overexpression of *Hnf1α, Hnf4α,* and *Hnf6* along with the hepatic maturation factors *ATF5, PROX1,* and *CEBPA* (Du et al., 2014). Synthetic-modified mRNAs have also been used to reprogram human fibroblasts to hepatocyte-like cells without genomic modification (Simeonov and Uppal, 2014). These hepatocyte-like cells derived from fibroblasts have similar functions as primary hepatocytes.

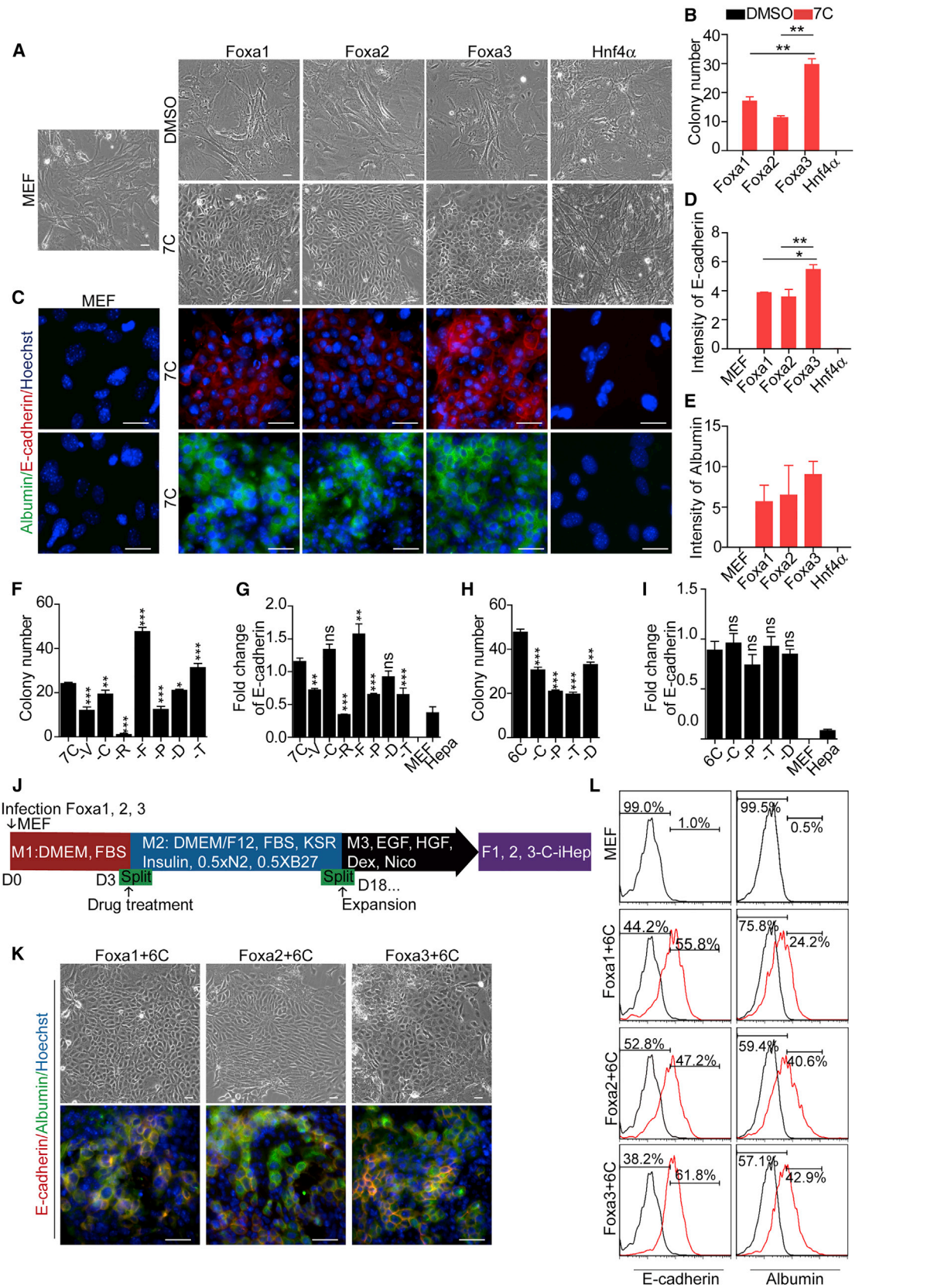

(legend on next page)

The hiHep-based bio-artificial liver system has been demonstrated to restore liver function and prolong survival in a porcine acute liver failure model (Shi et al., 2016).

Although effective in inducing hepatic transdifferentiation, viral vector-carried TFs are still not favored in therapeutic applications. Recent progress in chemical-mediated reprogramming and transdifferentiation have provided new ways of generating functional cells which might be safer in clinical use. Chemically induced pluripotent stem cells (CiPSCs) (Hou et al., 2013; Long et al., 2015), neural progenitor cells (Cheng et al., 2014), astrocytes (Tian et al., 2016), neurons (Zhang et al., 2015), and cardiomyocytes (CiCMs) (Fu et al., 2015) have been reported recently. Furthermore, two small molecules have been reported to improve iHep generation in the presence of *Hnf4α* and *Foxa3* (Lim et al., 2016).

The chemical cocktail CRFVPTD (C, CHIR99021; R, RepSox; F, Forskolin; V, VPA; P, Parnate; T, TTNPB; and D, Dznep) was originally reported to induce CiPSC generation from mouse embryonic fibroblasts (MEFs) without any TFs (Hou et al., 2013; Long et al., 2015). By fine-tuning the culture condition, we have demonstrated that this chemical cocktail is also able to induce MEF transdifferentiation into spontaneously beating CiCMs, with the minimal combination of CRFV (Fu et al., 2015). During our studies with CiPSCs or CiCMs, we have noticed that this chemical cocktail induces various morphological changes in MEFs, suggesting other transdifferentiation possibilities. Here, we report the generation and characterization of hepatocyte-like cells from mouse fibroblasts by chemical cocktails (most effective: CRVPTD) in combination with a single TF (*Foxa1, Foxa2,* or *Foxa3*).

RESULTS

Induction of Hepatocyte-like Cells from Fibroblasts by Single TF with Chemical Cocktails

To generate hepatocyte-like cells from mouse fibroblasts, two or three TFs involved in hepatocyte development are typically needed (Huang et al., 2011; Sekiya and Suzuki, 2011). *Hnf4α*, in combination with *Foxa1, Foxa2,* or *Foxa3*, has been reported to induce hepatic transdifferentiation of MEFs (Sekiya and Suzuki, 2011). However, all these TFs failed to induce any morphological changes in MEFs when expressed alone (Figure 1A). In contrast, if the single factor (*Foxa1, Foxa2,* or *Foxa3*)-transduced MEFs were treated with chemical cocktail CRFVPTD (7C), a number of colonies with epithelial morphology (in contrast to the mesenchymal morphology of MEFs) could be found (Figure 1A). These colonies could be observed as early as day 9 in *Foxa3*-transduced MEFs, while in *Foxa1*- or *Foxa2*-transduced MEFs, the colonies appeared at day 12 (Figure S1A). The epithelial morphology became very obvious at day 18 (Figures S1A, 1A, and 1B). Some of these colonies were E-cadherin- and albumin-positive (Figures 1C–1E). These colonies resemble induced hepatocyte-like cells reported previously (Huang et al., 2011; Sekiya and Suzuki, 2011), so we named them *Foxa1*-7C-iHeps, *Foxa2*-7C-iHeps, and *Foxa3*-7C-iHeps. However, no such colonies could be observed in *Hnf4α*-transduced MEFs even after 7C treatment (Figures 1A–1E).

We further optimized the chemical cocktail with the *Foxa3*-7C combination. We first determined the small molecules in the CRFVPTD cocktail critical for iHep induction by removing only one compound from the 7C set.

Figure 1. Hepatic Transdifferentiation of MEFs with One TF and Chemicals

(A) Representative morphologies after MEFs were transduced with *Foxa1, Foxa2, Foxa3,* or *Hnf4α* and treated with small molecules (CRFVPTD, 7C) or vehicle (DMSO), at day 18.

(B) Numbers of cell clusters with epithelial morphology presented in (A) at day 18. Data are representative of three independent experiments, means ± SEM (n = 3). $^{**}p < 0.01$.

(C) Immunofluorescent staining of E-cadherin and albumin in cell clusters generated from one TF-transduced MEFs treated with 7C or vehicle (DMSO). Nuclei are stained with Hoechst.

(D and E) Statistical data of the intensity of E-cadherin and albumin staining in (C). Data are means ± SEM (six random fields in a representative experiment of three independent experiments). $^{*}p < 0.05$, $^{**}p < 0.01$.

(F and G) Screening of compounds essential for hepatocyte-like cell induction by removing one compound from the 7C combinations. Number of the cell clusters with epithelial morphology (F) and qRT-PCR analysis of E-cadherin (G) are shown. Data are means ± SEM of three independent experiments. $^{*}p < 0.05$, $^{**}p < 0.01$, $^{***}p < 0.001$, versus 7C.

(H and I) Screening of compounds essential for hepatocyte-like cell induction by removing one compound from the 6C combinations. Number of the cell clusters with epithelial morphology (H) and qRT-PCR analysis of E-cadherin (I) are shown. Data are means ± SEM of three independent experiments. $^{**}p < 0.01$, $^{***}p < 0.001$, versus 6C.

(J) A schematic view of the optimized transdifferentiation protocol.

(K) The morphology and immunostaining of E-cadherin and albumin in *Foxa1*-6C-iHep, *Foxa2*-6C-iHep, and *Foxa3*-6C-iHep. Nuclei are stained with Hoechst.

(L) FACS analysis of E-cadherin^{+} and albumin^{+} cells induced by optimized condition at day 0 (MEF) or day 18 after induction. Representative plots from three independent experiments are shown.

Scale bars represent 50 μm. See also Figures S1 and S2.

Removing RepSox almost failed to induce any epithelial colonies, while removing VPA and Parnate significantly reduced the epithelial clusters. However, removing Forskolin increased the colony numbers (Figures 1F and S1B). qRT-PCR analysis of E-cadherin expression showed similar results (Figure 1G). By removing Forskolin, the 6C (CRVPTD) and *Foxa3* combination was very effective in generating the iHep colonies. Further removal of CHIR99021, Parnate, Dznep, or TTNPB from 6C reduced the colony numbers in all cases (Figures 1H, 1I, and S1C). These results suggest that V, C, R, P, D, and T are beneficial in generating iHeps.

Optimization of Culture Conditions and Preliminary Characterization of iHep Cells

A two-stage optimization strategy was carried out to improve the induction efficiency and promote the proliferation and maturation of single-TF-induced iHeps (Figure 1J). We first optimized the hepatic reprogramming medium (HRM) used in the first stage of the induction with CRVPTD (6C). Changing the basal medium from KnockOut-DMEM to DMEM/F12 significantly increased iHep induction. The addition of N2, B27, or insulin also increased the generation of epithelial clusters (Figures S1D and S1E). So, we combined these conditions and used this as the optimized induction condition (Figures S1F and S1G). Under the optimized induction condition, the iHep colonies could be observed as early as days 6–9 in all three groups (*Foxa1*-6C, *Foxa2*-6C, or *Foxa3*-6C) (Figure S2A), and many of the colonies were positive for both E-cadherin and albumin (Figure 1K). Fluorescence-activated cell sorting (FACS) analysis revealed that *Foxa1*-6C-iHep, *Foxa2*-6C-iHep, and *Foxa3*-6C-iHep were approximately 55.8%, 47.2%, and 61.8% positive for E-cadherin, and 24.2%, 40.6%, and 42.9% positive for albumin at day 18, respectively (Figure 1L). Hepatic genes including *AFP, Albumin, CK8, TTR, E-cadherin, Vitronectin, Cldn3, Hnf4α, Transferrin,* and *CK18,* and hepatic stem cell genes *CK19* and *EPCAM* were highly expressed in these *Foxa1*-6C-iHeps, *Foxa2*-6C-iHeps, or *Foxa3*-6C-iHeps at day 18 (Figure S2B). qRT-PCR also confirmed the time-dependent increase in the expression of hepatic-specific genes in *Foxa3*-6C-iHep, including *E-cadherin, albumin, CK8, Cldn3, Vitronectin,* and *CK18,* and hepatic stem cell markers *CK19* and *EPCAM* (Figure S2C).

For further characterization, these iHeps were passaged onto new dishes with hepatocyte-maintaining medium (HMM, after day 18). In addition to the 6C, the HMM was supplemented with dexamethasone, nicotinamide, epidermal growth factor (EGF), and hepatocyte growth factor (HGF), which have been reported to be beneficial for hepatocyte culture (Jia, 2011). The final optimized protocol is described in the Experimental Procedures and summarized in Figure 1J. The *Foxa3*-6C-iHep cells were stably expandable *in vitro* and displayed a typical S-shaped growth curve (Figure S2D). The mean population doubling time of *Foxa3*-6C-iHeps was approximately 24 hr, and this growth speed could be maintained to at least 30 passages. In contrast, the growth of MEFs was significantly reduced at passage 4 (Figure S2D). PCR analysis showed that the hepatic genes were also highly expressed in the P30-*Foxa3*-6C-iHep (Figure S2E).

iHeps Generated with Single TF and Chemicals Did Not Pass an iPSC Stage

To answer the question whether the single factor-iHeps go through an iPSC-like stage, we did a parallel comparison between iPSC induction and iHep induction with OG2 MEFs, which contain an *Oct4*:GFP reporter (Wang et al., 2011; Xu et al., 2013). Time-lapse imaging clearly showed the emergence of GFP$^+$-iPSC colonies in Yamanaka factor (*Oct4, Klf4,* and *Sox2*)-mediated reprogramming as early as day 6 (Figure S3A). In contrast, in the *Foxa1*-6C, *Foxa2*-6C, and *Foxa3*-6C groups, the hepatocyte-like colonies could be observed from days 6 to 9, but no GFP$^+$ colonies appeared (Figure S3A). qRT-PCR analysis also revealed the time-dependent increase in the expression of pluripotency genes such as *Oct4, Sox2, Nanog,* and *Rex1* during iPSC induction, but in *Foxa1*-6C-, *Foxa2*-6C-, and *Foxa3*-6C-mediated iHep induction, the pluripotency genes remained at very low levels during the whole process (Figure S3B).

Previous studies have shown that *Foxa* genes were important in the development of liver and pancreas (Costa et al., 2003). To test whether *Foxa1*-6C, *Foxa2*-6C, and *Foxa3*-6C could also induce the generation of pancreatic progenitor- or pancreatic-like cells, the expression level of pancreatic progenitor makers such as *Pdx1, Pax6, Ngn3, Nkx6.1,* and *Isi1*, and the mature pancreatic cell markers, *Insulin1* and *Insulin2* (Cerda-Esteban et al., 2017), were also analyzed with qRT-PCR. As demonstrated in Figure S3C, all pancreatic-related makers remained at a very low level. A number of genes that have been detected in both pancreatic progenitors and liver, such as *MafA, Hhex,* and *Prox1* (Cerda-Esteban et al., 2017; Huang et al., 2014), were found to increase in a time-dependent way during iHep induction; and, at day 18, the expression of those three genes in the iHep induction systems were similar to hepatocytes. Moreover, the intestinal genes such as *Secretin* and *Chromogranin A* were not detected (Figure S3C).

Lineage Tracing of Single-TF Transdifferentiation of MEFs to iHeps

To avoid possible contamination of hepatic progenitor cells in the MEFs, a lineage-tracing experiment was carried out to track the origin of the *Foxa3*-6C-iHeps. The R26R^{tdTomato}

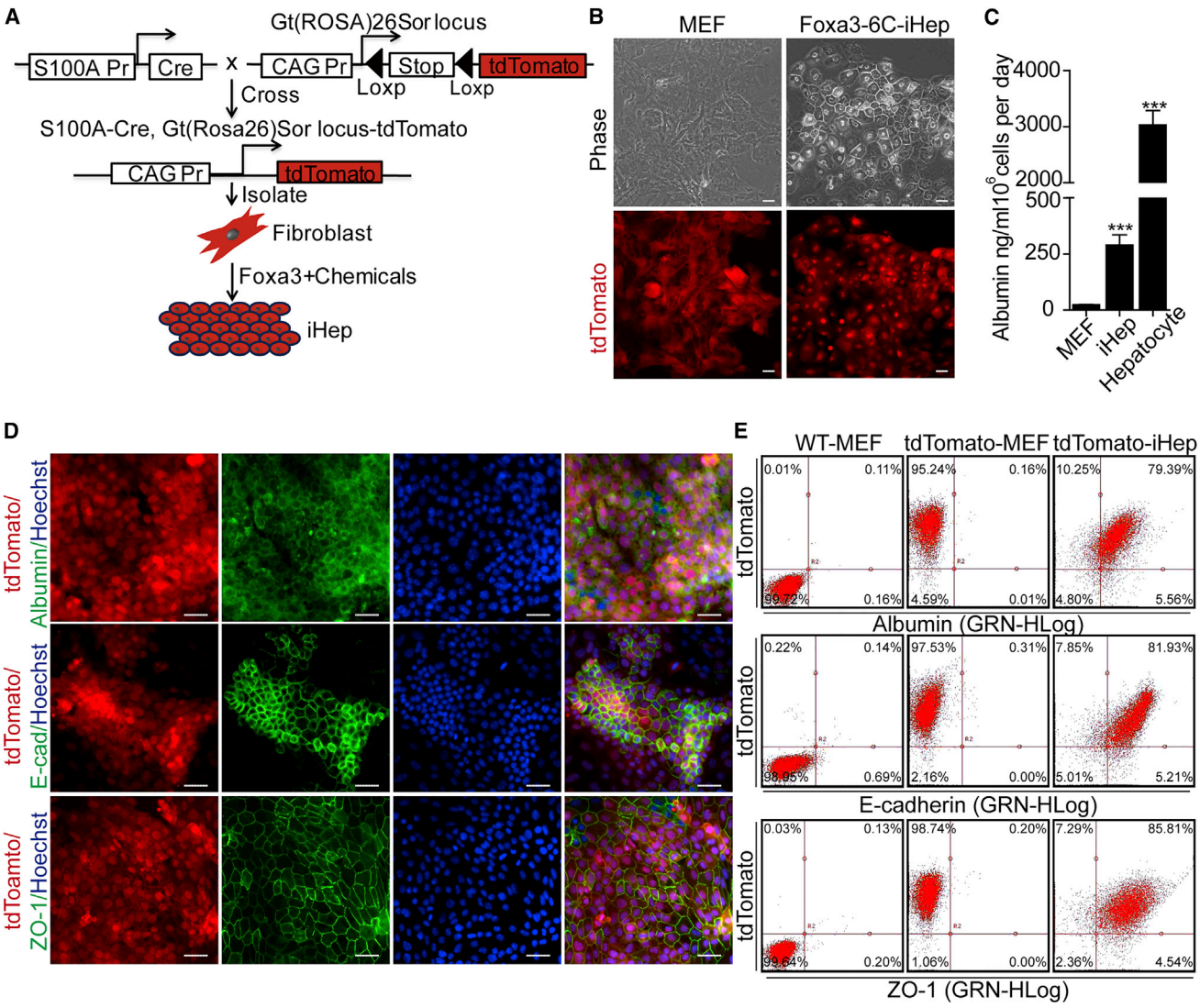

Figure 2. Lineage Tracing of *Foxa3*-6C-Induced Transdifferentiation of MEFs toward Hepatocyte-like Cells

(A) Schematic diagram of the genetic fate mapping method used to trace the origin of hepatocyte-like cells reprogrammed from *Fsp1*-Cre:R26R^{tdTomato} MEFs.

(B) Representative morphologies of *Fsp1*-Cre:R26R^{tdTomato} MEFs and *Foxa3*-6C-iHeps induced from these MEFs.

(C) ELISA analysis of the secreted albumin in the media culturing MEFs, *Foxa3*-6C-iHeps, and primary hepatocytes. Data are means ± SEM of three independent experiments. ***$p < 0.001$ versus MEFs.

(D) Immunofluorescent staining of hepatic markers, including albumin, E-cadherin, and ZO-1 in tdTomato$^+$-*Foxa3*-6C-iHeps. Nuclei are stained with Hoechst.

(E) FACS analyses of E-cadherin$^+$, albumin$^+$, and ZO-1$^+$ cells presented in (D), wild-type MEFs (WT-MEF) from C57 mice and tdTomato-MEFs were used as control. Representative plots from three independent experiments are shown.

Scale bars represent 50 μm. See also Figure S4.

mice, in which tdTomato expression is prevented by a *loxP*-flanked STOP cassette, were crossed with the *Fsp1*-Cre mice. Since *Fsp1* is specifically expressed in fibroblasts (Bhowmick et al., 2004), the offspring (*Fsp1*-Cre:R26R^{tdTomato}) would have the tdTomato expressed specifically in the fibroblasts (Figure 2A).

The *Fsp1*-Cre:R26R^{tdTomato} (tdTomato$^+$) MEFs were isolated and induced with *Foxa3* plus 6C. Epithelial clusters with the expression of tdTomato could also be observed in the culture (Figure 2B). We passaged the tdTomato$^+$-*Foxa3*-6C-iHeps and cultured them in HMM for further experiments (after day 18 of induction). TdTomato$^+$-*Foxa3*-6C-iHeps passaged

for three to five times in HMM were used for the following analysis. Albumin could be detected in medium culturing these iHep cells (Figure 2C). Immunofluorescence analysis confirmed that these tdTomato$^+$-*Foxa3*-6C-iHeps were positive for hepatocyte markers albumin, E-cadherin, and ZO-1 (Figure 2D). FACS analysis revealed that approximately 79.39%, 81.93%, or 85.81% of the tdTomato$^+$-*Foxa3*-6C-iHep were positive for albumin, E-cadherin, and ZO-1, respectively (Figure 2E). Ten tdTomato$^+$-*Foxa3*-6c-iHep clones were established, and PCR analysis showed that they expressed most of the hepatic genes, but not the fibroblast markers (Figures S4A and S4B). Immunostaining also confirmed the loss of *α-SMA* in the tdTomato$^+$-*Foxa3*-6c-iHep cells (Figure S4C).

Hepatic Functions of iHep Cells Generated from MEFs

Foxa3-6C-iHeps or tdTomato$^+$-*Foxa3*-6C-iHeps passaged for three to five times in HMM were used for further functional characterization. Similar to hepatocytes, Periodic acid-Schiff (PAS) staining showed glycogen stores in the *Foxa3*-6C-iHep cells, and these *Foxa3*-6C-iHeps were able to intake low-density lipoprotein (LDL) (Figure 3A). Moreover, PCR analysis revealed that a number of important hepatic Cyp450 enzymes, including *Cyp1a1, Cyp1a2, Cyp2b10, Cyp2c29, Cyp2c38, Cyp2d22, Cyp2e1, Cyp3a11,* and *Cyp3a13,* were highly expressed in tdTomato$^+$-*Foxa3*-6C-iHeps (Figure 3B). The proteins of Cyp1a2, Cyp2c9, and Cyp2c19 were also confirmed by immunofluorescent staining in tdTomato$^+$-*Foxa3*-6C-iHeps (Figure 3C). Importantly, the metabolic products of phenacetin (acetaminophen), tolbutamide (hydroxy-tolbutamide), testosterone (6β-OH-testosterone), and diclofenac (4′-OH-diclofenac) were all detectable in the media culturing tdTomato$^+$-*Foxa3*-6C-iHeps (Figure 3D), indicating the acquisition of specific drug metabolism enzymes or pathways. Taken together, these results demonstrate that the iHeps induced by *Foxa3* and 6C possess typical functional features of hepatocytes.

iHep Induction from Tail-Tip Fibroblasts

To explore whether the condition we used to generate iHeps from MEFs could be used to induce iHeps from adult fibroblasts, tdTomato$^+$-TTFs (tail-tip fibroblasts) were isolated and induced with *Foxa3* plus 6C under the optimized conditions. The transdifferentiation process of TTFs was slower than MEFs. A number of colonies with epithelial morphology could be found 4 weeks later (Figures 4A and 4B). These epithelial-like tdTomato$^+$ colonies were picked and expanded in HMM for further characterization. Immunofluorescent staining confirmed the loss of α-SMA in these tdTomato$^+$-*Foxa3*-6C-TTF-iHep cells (Figure S5A). PAS staining also showed glycogen stores in the tdTomato$^+$-*Foxa3*-6C-TTF-iHeps (Figure 4C). Albumin could also be detected in medium culturing these iHep cells (Figure S5B). PCR analysis revealed that hepatic genes, including *E-cadherin, Albumin, ZO-1, CK8, CK18, TTR, Vitronectin, Transferrin, Cldn3, Hnf4α,* and *AFP,* and hepatic stem cell marker, *EPCAM*, were also expressed in these *Foxa3*-6C-TTF-iHeps (Figure S5C). Immunofluorescent staining also confirmed that these tdTomato$^+$-*Foxa3*-6C-TTF-iHeps were positive for albumin, E-cadherin, and ZO-1 (Figure 4D).

PCR analysis also revealed that the genes of a number of important hepatic Cyp450 enzymes, including *Cyp1a1, Cyp2b10, Cyp2c29, Cyp2c38, Cyp3a13, Cyp3a41, Cyp2d22, Cyp2e1,* and *Fah,* were highly expressed in tdTomato$^+$-*Foxa3*-6C-TTF-iHeps (Figure S5C). The proteins of Cyp1a2, Cyp2c9, and Cyp2c19, and fumarylacetoacetate hydrolase (Fah), were also detected in tdTomato$^+$-*Foxa3*-6C-TTF-iHeps with immunofluorescent staining (Figure 4E). In the functional assay of Cyp450, the metabolic products of phenacetin (acetaminophen), tolbutamide (hydroxytolbutamide), testosterone (6β-OH-testosterone), and diclofenac (4′-OH-diclofenac) were all detectable in the media culturing tdTomato$^+$-*Foxa3*-6C-TTF-iHeps (Figure 4F).

iHep Cells Can Exert Hepatic Function in *Fah*-Deficient Mice and Save Their Lives

Fah is involved in the catabolism of the amino acids phenylalanine and tyrosine. Mutation or deletion of the *Fah* gene leads to tyrosinemia and hepatic necrosis. *Fah*$^{-/-}$ mice need to be supplemented with 2-(2-nitro-4-trifluoro-methylbenzyol)-1,3-cyclohexanedione (NTBC) or transplantation of primary hepatocytes for survival (Grompe et al., 1993). This is an ideal model to evaluate whether the iHeps can function as hepatocytes *in vivo*.

To generate traceable primary hepatocytes, which were used as positive control for transplantation, the R26R^{tdTomato} mice were crossed with the *albumin*-Cre mice. The hepatocytes of the progeny expressed tdTomato. After NTBC withdrawal, tdTomato$^+$-MEFs, tdTomato$^+$-*Foxa3*-6C-iHeps, or tdTomato$^+$-hepatocytes were transplanted into *Fah*$^{-/-}$ mice via intra-splenic injection through a left-flank incision under tribromoethanol anesthesia. All of the eight *Fah*$^{-/-}$ mice transplanted with tdTomato$^+$-MEFs (MEF-*Fah*$^{-/-}$) died within 5 weeks after NTBC withdrawal, and their livers showed severe inflammation and necrosis (Figures 5A and 5B). In contrast, 6 of 8 *Fah*$^{-/-}$ mice transplanted with primary hepatocytes survived (hepatocyte-*Fah*$^{-/-}$). It was exciting to find that four of the 12 *Fah*$^{-/-}$ mice transplanted with tdTomato$^+$-*Foxa3*-6C-iHeps (iHep-*Fah*$^{-/-}$) were alive 8 weeks after NTBC withdrawal, and the survivors' livers were as normal as the livers of the surviving hepatocyte-transplanted *Fah*$^{-/-}$ mice (Figures 5A and 5B). Under the fluorescent microscope, tdTomato$^+$-*Foxa3*-6C-iHeps and tdTomato$^+$

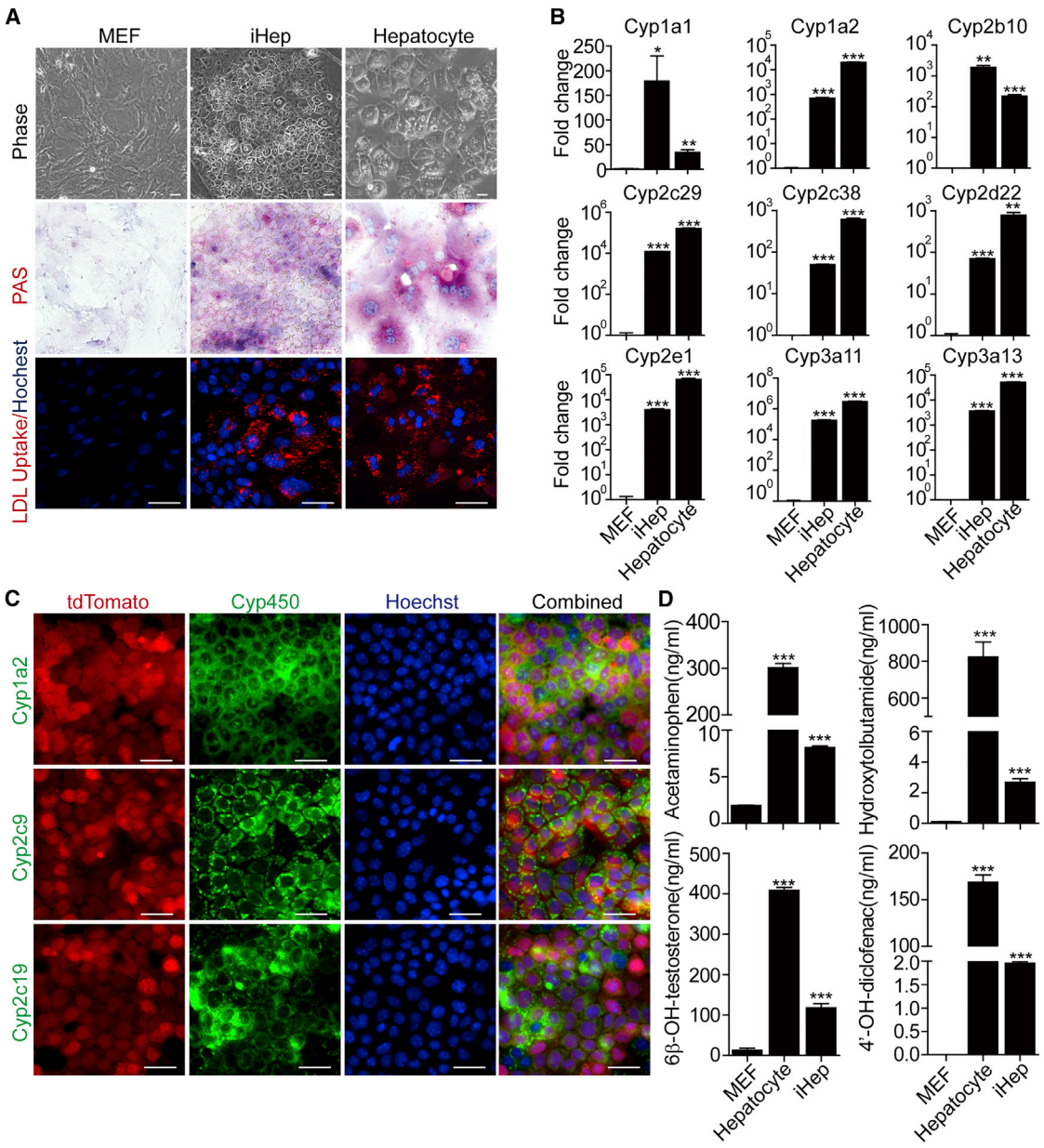

Figure 3. Characterization of iHep Cells *In Vitro*

(A) PAS staining and Dil-ac-LDL (red fluorescence) uptake assay performed in MEFs, *Foxa3*-6C-iHeps, and primary hepatocytes. Nuclei are stained with Hoechst.

(B) qRT-PCR analysis of the expression of hepatic Cyp450 genes. Data are means ± SEM of three independent experiments. *$p < 0.05$, **$p < 0.01$, ***$p < 0.001$ versus MEFs.

(C) Immunofluorescent staining of hepatic Cyp450 enzyme, Cyp1a2, Cyp2c9, and Cyp2c19 in td-Tomato^{+}-Foxa3-6C-iHep generated from *Fsp1*-Cre:R26R^{tdTomato} MEFs. Nuclei are stained with Hoechst.

(D) Drug metabolism ability of *Foxa3*-6C-iHeps. Four drugs (phenacetin, tolbutamide, testeone, and diclofenac) and their metabolic products (acetaminophen, hydroxytolbutamide, 6β-OH-testosterone, and 4′-OH-diclofenac) were measured by liquid chromatography-tandem mass spectrometry. Data are means ± SEM of three independent experiments. ***$p < 0.001$ versus MEFs.

Scale bars represent 50 μm.

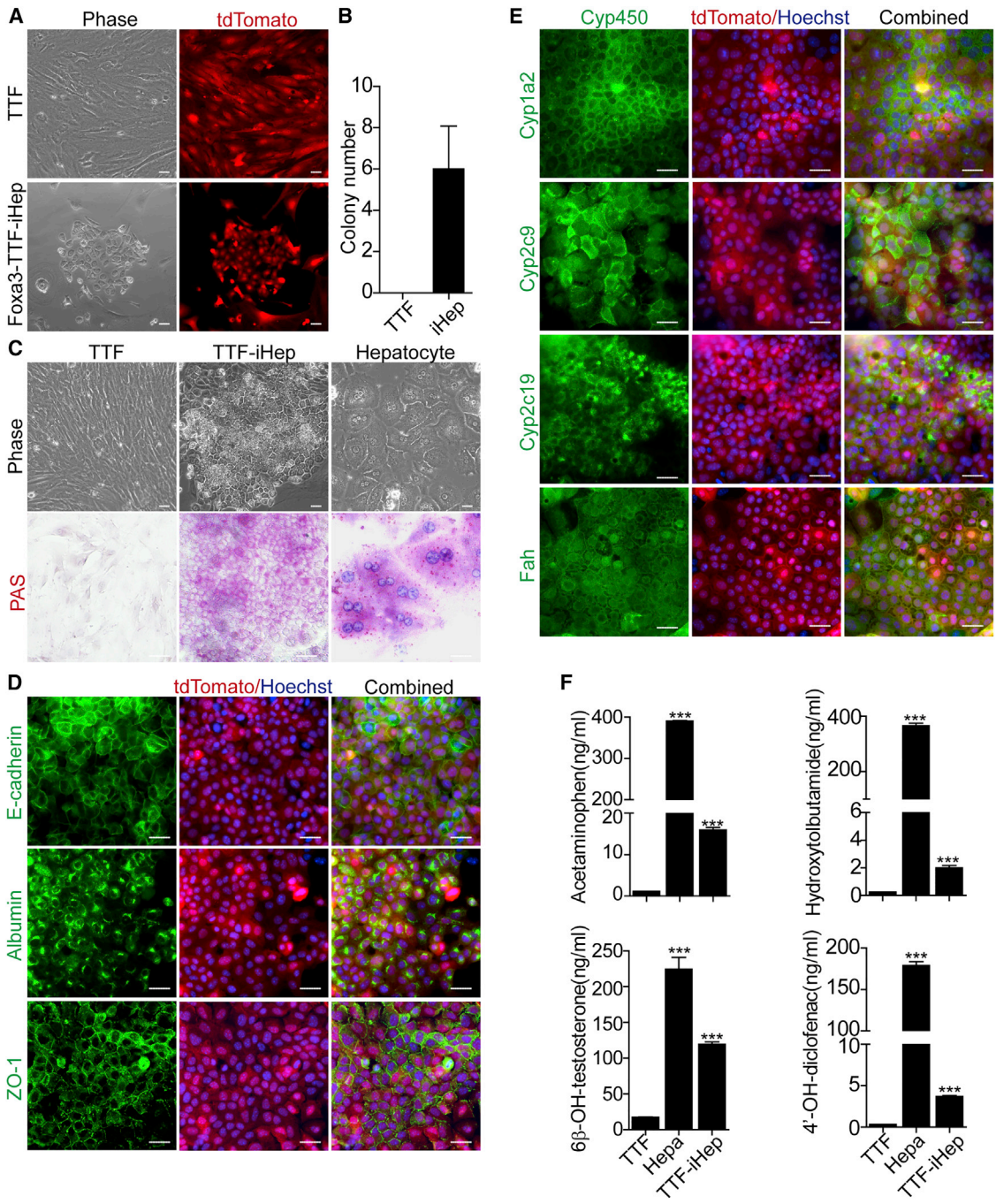

Figure 4. Hepatic Transdifferentiation of TTF

(A) Representative morphologies of tdTomato$^+$-*Foxa3*-6C-TTF-iHeps after a 4-week induction.

(B) Number of epithelial-like colonies after a 4-week induction with 100,000 cells starting TTFs. Data are means ± SEM of three independent experiments.

(C) Representative morphologies and PAS staining of TTFs, tdTomato$^+$-*Foxa3*-6C-TTF-iHeps, and primary hepatocytes.

(D) Immunofluorescent staining of hepatic markers, including E-cadherin, albumin, and ZO-1 in tdTomato$^+$-*Foxa3*-6C-TTF-iHeps. Nuclei are stained with Hoechst.

(E) Immunofluorescent staining of hepatic Cyp450 enzyme including Cyp1a2, Cyp2c9, and Cyp2c19, and Fah, in TTF-iHeps. Nuclei are stained with Hoechst.

(legend continued on next page)

hepatocytes could be easily observed in livers of the surviving animals (Figure 5B). Both repopulated *Foxa3*-6C-iHeps and primary hepatocytes expressed albumin and Fah in the liver of *Fah*$^{-/-}$ mice (Figures 5C and 5D). Serum levels of total bilirubin, alanine transaminase (ALT), aspartate transaminase (AST), and alkaline phosphatase were markedly reduced in both the hepatocyte-*Fah*$^{-/-}$ and iHep-*Fah*$^{-/-}$ mice compared with the MEF-*Fah*$^{-/-}$ mice (Figure 5E). These data demonstrate that *Foxa3*-6C-iHeps can exert hepatic function *in vivo* and prolong the life of *Fah*$^{-/-}$ mice after NTBC withdrawal.

DISCUSSION

In this study, we demonstrated that *Foxa1, Foxa2,* or *Foxa3* alone is sufficient for generating *in vitro* expandable and *in vivo* functional iHeps in the presence of the chemical cocktail CRVPTD. Although previous investigations have showed that functional iHeps can be induced from mouse fibroblasts by ectopic expression of TFs (Huang et al., 2011; Sekiya and Suzuki, 2011), and small molecules can facilitate factor-mediated hepatic transdifferentiation (Lim et al., 2016), it is still worthy of our efforts to find chemical cocktails to replace the role of TFs in cell transdifferentiation. Compared with previous methods, our iHeps can be easily generated and is one step closer to the TF-free iHeps which might be more amendable in clinical applications.

The precise mechanisms underlying the chemical induction of hepatic transdifferentiation remain to be elucidated. It has been reported that the chemical combination CRFVPTD could lead to both CiPSCs and CiCMs under different culture conditions. In our CiCM study, we found that the chemical cocktail induced a number of morphological changes in MEF culture and proposed a mix progenitor theory (Fu et al., 2015). Indeed, under hepatocyte culture conditions, this cocktail successfully induced iHeps with one TF (*Foxa1, Foxa2,* or *Foxa3*). A previous study indicated a minimal of two TFs (*Hnf4α* in combination with *Foxa1, Foxa2,* or *Foxa3*) is necessary to induce hepatic transdifferentiation of MEFs (Sekiya and Suzuki, 2011). The chemical cocktail reported here is able to replace *Hnf4α*, but not *Foxa1, Foxa2,* or *Foxa3*.

Hnf4α is a master regulator for hepatocyte differentiation, liver development, and maintenance of liver functions (Lu, 2016). *Hnf4α*$^{-/-}$ embryos exhibit a severe visceral endoderm defect, preventing gastrulation and causing a failure of development past 6.5 dpc (Chen et al., 1994). Later studies in adult mice with liver-specific deletion of *Hnf4α* revealed that this TF is essential in regulating the expression of key genes in drug metabolism, bile acid synthesis, lipid homeostasis, gluconeogenesis, ureagenesis, cell adhesion, proliferation, and apoptosis in hepatocytes (Lu, 2016). One of the most important cellular phenomena mediated by Hnf4α is EMT/MET (epithelial-to-mesenchymal transition/mesenchymal-to-epithelial transition). Hnf4α is a dominant regulator of the epithelial phenotype (Niehof and Borlak, 2009; Parviz et al., 2003) and directly inhibits the master EMT regulators and mesenchymal gene expression (Santangelo et al., 2011). The EMT in hepatocyte correlates with the downregulation of Hnf4α (Cicchini et al., 2006). MET is a key element in cellular reprogramming, including the generation of iPSCs and iHeps (Li et al., 2010; Lim et al., 2016). In our chemical combination, RepSox is a transforming growth factor β inhibitor that facilitates the MET process. This is probably why *Hnf4α* can be replaced by this chemical cocktail. Removal of RepSox results in dramatically reduced hepatic reprogramming efficiency, further demonstrating the importance of the MET process.

Like many TFs, the transcription activity of Hnf4α is regulated by a number of post-translational modifications, including methylation, acetylation, and phosphorylation. In particular, Hnf4α is phosphorylated at S142 and S143 by the cAMP-PKA pathway in liver, and such modification decreased Hnf4α-mediated transcription of L-type pyruvate kinase (Viollet et al., 1997). This is possibly why removing Forskolin, which induces the elevation of intracellular cAMP and may reduce the transcriptional activity of endogenous Hnf4α, is beneficial in inducing hepatic transdifferentiation of MEFs. However, the regulation of Hnf4α by PKA might be more complex and is cell-context dependent: cAMP-PKA inhibits the transcriptional activity of HNF4α in COS-1 cells, whereas, in HepG2 cells, a stimulatory effect is observed due to the induction of PGC1α by cAMP (Dankel et al., 2010).

While successfully replacing *Hnf4α* with the chemical cocktail, we failed to replace the other TF (*Foxa1, Foxa2,* or *Foxa3*). Foxa family members share >90% homology in their amino acid sequence in the winged helix domains and they bind to similar DNA target sequences within hepatocyte-specific regulatory regions (Friedman and Kaestner, 2006). The Foxa2 gene is first in the family to be activated during embryogenesis, at embryonic day 6.5 (E6.5), in the anterior primitive streak (Sasaki and Hogan, 1993). The expression of Foxa1 is first detectable at E7.0 in the

(F) Drug metabolism ability of tdTomato^{+}-*Foxa3*-6C-TTF-iHeps. Four drugs (phenacetin, tolbutamide, testeone, and diclofenac) and their metabolic products (acetaminophen, hydroxytolbutamide, 6β-OH-testosterone, and 4′-OH-diclofenac) were measured by liquid chromatography-tandem mass spectrometry. Data are means ± SEM of three independent experiments. ***$p < 0.001$ versus TTFs.
Scale bars represent 50 μm. See also Figure S5.

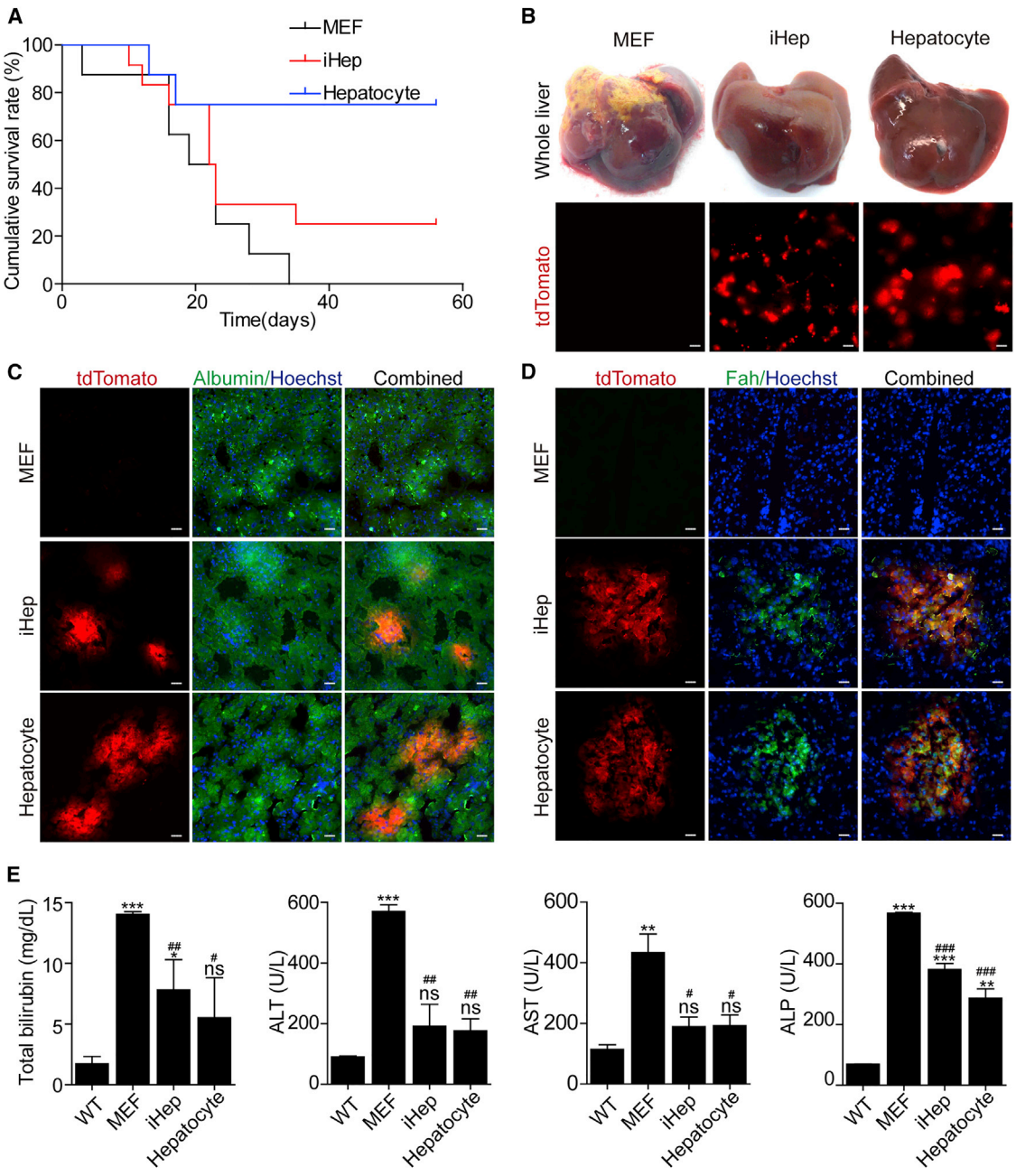

Figure 5. iHep Cells Rescue *Fah*-Deficient Mice and Support Hepatic Function *In Vivo*

(A) Kaplan-Meier survival curve of *Fah*$^{-/-}$ mice transplanted with tdTomato^{+}-MEF (n = 8), tdTomato^{+}-*Foxa3*-6C-iHeps (n = 12), and tdTomato^{+}-hepatocytes (n = 8) after NTBC withdrawal.

(B) Representative pictures of whole liver (top) and tdTomato images of the liver transplanted with tdTomato^{+}-MEF, tdTomato^{+}-*Foxa3*-6C-iHeps, or td-Tomato^{+}-hepatocytes (bottom).

(C and D) Immunofluorescent staining of albumin or Fah in frozen sections of liver isolated from *Fah*$^{-/-}$ mice transplanted with tdTomato^{+}-MEF, tdTomato^{+}-*Foxa3*-6C-iHeps, or tdTomato^{+}-hepatocytes.

(E) The amounts of ALP, total bilirubin, ALT, and AST in the plasma of WT mice, *Fah*$^{-/-}$ mice transplanted with tdTomato^{+}-MEF, tdTomato^{+}-*Foxa3*-6C-iHeps, or tdTomato^{+}-hepatocytes. Data are means ± SEM, n = 3. $^{*}p < 0.05$, $^{**}p < 0.01$, $^{***}p < 0.001$ versus WT. $^{\#}p < 0.05$, $^{\#\#}p < 0.01$, $^{\#\#\#}p < 0.001$ versus MEFs. Scale bars represent 250 μm in (B), 50 μm in (C and D). ALT, alanine transaminase; AST, aspartate transaminase; ALP, alkaline phosphatase.

later primitive streak (Monaghan et al., 1993). Foxa3, the most highly expressed of the three in the adult liver, is first detectable at E8.5 in the region extending from the hindgut-foregut boundary (Monaghan et al., 1993). Gene ablation studies of Foxa factors in mice have shown that Foxa1 and Foxa2 redundantly regulate liver development and metabolism; deletion of Foxa3 in the liver caused compensatory increases in levels of Foxa1 and Foxa2, but the hepatic role of Foxa3 is unclear (Kaestner et al., 1998; Lee et al., 2005). The structures of the Foxas are similar to linker histone H1, and the Foxa proteins are able to open highly compacted chromatin *in vitro* without the SWI/SNF chromatin remodeling complex (Cirillo et al., 2002). Consequently, the Foxa proteins have been reported to act as "pioneer" TFs, displacing linker histones from compacted chromatin and facilitating the binding of other TFs. In liver development, Foxa can direct target genes and activate liver-specific genes, but not through any specific signaling pathway (Friedman and Kaestner, 2006). This is possibly why Foxas are always used in hepatic transdifferentiation in both human and mouse systems, and is not easy to be replaced by chemicals. A recent study (Lim et al., 2016) has reported that *Hnf1α* (or *Hnf4α*) alone can induce mature iHeps in the presence of chemicals (A83-01, CHIR99021) and bone morphogenetic protein 4. Unfortunately, the combination of their conditions and our cocktail failed to generate full-chemical iHeps from mouse fibroblasts. In the future, more studies will be needed to identify cytokines, growth factors, or chemicals that can replace both families of TFs simultaneously in converting fibroblasts into hepatocytes.

Another interesting property of our one-TF-iHeps generated with the chemical cocktail is that they can be expanded by more than 30 passages. Although adult hepatocytes have a remarkable ability to proliferate *in vivo*, it is difficult to expand functional hepatocytes *in vitro*. It has been reported that oxygenated or microfabricated co-cultures could stabilize metabolic functions of primary hepatocytes for a few weeks (Khetani and Bhatia, 2008; Kidambi et al., 2009), but not the proliferative capacity of the cells. Small-molecule approaches only enable about ten passages of human hepatocytes and long-term storage of the cells is very difficult (Levy et al., 2015). Our iHeps are functional *in vivo* to a certain extent, but compared with the primary hepatocytes there are still some gaps, such as the expression level of hepatic feature genes, the ability of drug metabolism, and the *in vivo* repopulation ability and functions. Therefore, there might be a balance between maturity and expandability in hepatocytes.

In conclusion, we generate functional and expandable hepatocytes using a single TF plus a chemical cocktail, and are one step closer to the TF-free iHeps. More compounds and culture conditions should be screened and optimized to replace the last TF and to improve the maturity of iHeps. The chemicals used in iHep induction may also be used to facilitate the expanding and long-term culture of primary hepatocyte *in vitro*.

EXPERIMENTAL PROCEDURES

All experimental procedures for the use and the care of animals complied with international guidelines for the care and use of laboratory animals and were approved by the Animal Ethics Committee of Shanghai Institute of Materia Medica.

Derivation of Fibroblasts and Cell Culture

MEFs were isolated from E12.5. Gonads and internal organ were removed before processing for isolation of MEF cells. MEFs were growth in fibroblast growth medium (FGM) consisting of DMEM (Gibco), 15% fetal bovine serum (FBS, Gibco), 2 mM GlutaMAX (Gibco), 0.1 mM non-essential amino acids (NEAA) (Gibco), 100 units/mL penicillin, and 100 μg/mL streptomycin. For lineage-tracing experiments the *Fsp1*-Cre mice (Jackson Laboratory) were mated with $R26R^{tdTomato}$ mice (Jackson Laboratory) and isolated the Fsp1-Cre:$R26R^{tdTomato}$ (td-tomato-positive) MEFs from E12.5. $TdTomato^{+}$-TTFs were isolated from adult (8–10 weeks) *Fsp1*-Cre:$R26R^{tdTomato}$ mice. Tail tips were cut into pieces and then dispersed on gelatin-coated 10 cm culture dishes containing 2 mL FGM, and an additional 8 mL FGM was supplemented on the next day.

Primary Hepatocyte Isolation and Culture

Primary hepatocytes were isolated by a standard two-step collagenase perfusion method. In brief, the liver was perfused through the inferior vena with Perfusion buffer I (0.5 mM EGTA, 16 mM $NaHCO_3$, Hank's balanced salt solution (HBSS) without Ca^{2+} and Mg^{2+}) for about 30 mL, and then perfused with Perfusion buffer II (0.4 mg/mL collagenase type IV [Gibco], 10 mM HEPES, 16 mM $NaHCO_3$, 1× HBSS with 5 mM Ca^{2+} and 1.2 mM Mg^{2+}) for 25 mL. After the perfusion, the liver was removed from the abdominal cavity and hepatocytes were released into the DMEM medium using sterile surgical scissors. Cell suspension was filtered through a 350 μm cell strainer. Hepatocytes were purified with Percoll buffer (50% Percoll [Sigma-Aldrich], 50% DMEM) at low-speed centrifugation (1,500 rpm, 15 min). Viability of isolated hepatocytes was around 90% as determined by trypan blue. Primary hepatocytes were cultured in hepato-medium consisting of DMEM/F12 (Gibco), 10% FBS, 1 μg/mL insulin (Sigma-Aldrich), 100 nM dexamethasone (Sigma-Aldrich), 10 mM nicotinamide (Sigma-Aldrich), 2 mM GlutaMAX, 0.1 mM NEAA, 100 units/mL penicillin, 100 μg/mL streptomycin, 20 ng/mL EGF (Sigma-Aldrich), and 20 ng/mL HGF (Gibco).

Generation of iHep

Retroviruses were produced by transfection of Plat-E cells with pGCDNsam retroviral vectors containing the coding sequences of mouse *Foxa1, Foxa2, Foxa3,* or *Hnf4α* (Addgene). MEFs were seeded at a density of 200,000 cells per well in 6-well plates and cultured in FGM overnight. Then the medium was replaced by

virus-containing supernatant supplemented with 4 μg/mL polybrene, and the plates were centrifuged at 2,500 rpm for 90 min to ensure viral infection. Medium was changed into fresh FGM immediately after virus transduction. Two days post viral infection, MEFs were trypsinized into single cells and reseeded at a density of 100,000 cells per well on 12-well plates. Next day, the medium was changed to HRM (DMEM/F12, 10% FBS, 10% KSR [Gibco]). Insulin (1 μg/mL), 0.5× N2, 0.5× B27 (Gibco), 2 mM GlutaMAX, 0.1 mM NEAA, 100 units/mL penicillin, and 100 μg/mL streptomycin, containing the small-molecule cocktails CRFVPTD or CRVPTD (10 μM CHIR99021 [C], 10 μM RepSox [R], 0.5 mM VPA [V], 5 μM Parnate [P], 1 μM TTNPB [T], 50 μM Forskolin [F], and 50 nM Dznep [D]). At day 18, the cells were reseeded onto new 6-well plates, and the medium was changed to hepatocyte expansion medium (DMEM/F12, 10% FBS, 10% KSR, 1 μg/mL insulin, 100 nM dexamethasone, 10 mM nicotinamide, 2 mM GlutaMAX, 0.1 mM NEAA, 100 units/mL penicillin, 100 μg/mL streptomycin, 20 ng/mL EGF, and 20 ng/mL HGF) (Gibco) supplemented with the chemical cocktail CRVPTD.

Mouse iPSC Generation

Mouse iPSCs were induced as reported previously (Wang et al., 2011; Xu et al., 2013). In brief, the retrovirus containing the coding sequences of mouse *Oct4, Sox2,* and *Klf4* was produced by transfection of Plat-E cells with pMXs retroviral vectors (Addgene). OG2 MEFs (MEFs containing an *Oct4*:GFP reporter) were infected with the virus-containing *Oct4, Sox2,* and *Klf4*. Two days post virus infection, MEFs were trypsinized into single cells and reseeded at a density of 20,000 cells per well on 12-well plates pre-seeded with irradiated MEF feeders, supplemented with mES medium (DMEM supplemented with 15% FBS, 2 mM GlutaMAX, 0.1 mM NEAA, 0.1 mM β-mercaptoethanol 1,000 U/mL leukemia inhibitory factor [LIF], 100 units/mL penicillin, and 100 μg/mL streptomycin); this day was counted as day 0. At day 3 to day 18, the culture medium was replaced with KSR medium (KnockOut-DMEM supplemented with 15% knockout serum replacement, 2 mM GlutaMAX, 0.1 mM NEAA, 0.1 mM β-mercaptoethanol, 1,000 U/mL LIF, 100 units/mL penicillin, and 100 μg/mL streptomycin).

Immunofluorescence Staining

Cells were fixed with 4% paraformaldehyde (PFA) for 30 min at room temperature, after being washed with PBS three times, the cells were blocked and permeated with PBS containing 5% BSA and 0.3% Triton for 1 hr at room temperature. Then cells were incubated with the relevant primary antibody at 4°C overnight. After a thorough washing, cells were incubated with the appropriate fluorescence-conjugated secondary antibody for 1 hr at room temperature. Nuclei were stained with Hoechst 33,342 (10 μg/mL).

For staining of frozen tissue sections, fresh liver specimens were embedded in cryo-embedding medium and stored in frozen blocks at −80°C prior to sectioning. Sections of 10 μm thickness were fixed with 4% PFA for 30 min, and then blocked with 5% BSA. The sections were then incubated with the correct primary antibodies and secondary antibodies similar to cell staining. Nuclei were stained with Hoechst 33,342 (10 μg/mL). Images were captured with an Olympus IX71 inverted fluorescent microscope. Antibodies used in this study are as follows: anti-E-cadherin (CST, 24E10), anti-albumin (Bethyl Laboratories, A90-234A), anti-ZO-1 (Gibco, 40–2200), anti-Cyp1a2 (Abcam, ab22717), anti-Cyp2c9 (Abcam, ab4236), anti-Cyp2c19 (Abcam, ab137015), and anti-Fah (Abcam, ab81087).

PAS Stain and DiI-ac-LDL-Uptake Assay

To analyze the glucose storage ability of iHeps, iHeps were fixed by 4% PFA and stained with the PAS Kit (Sigma) according to the manufacturer's instructions. LDL-uptake ability was measured by culturing MEF, iHeps, and primary hepatocyte in DMEM/F12 containing DiI-Ac-LDL (10 μg/mL) for 4 hr at 37°C. Nuclei were stained by Hoechst and images were captured with an Olympus IX71 inverted fluorescent microscope.

Albumin ELISA and Cyp450 Metabolism Assay

To analyze the ability for albumin secretion, MEFs, iHeps, and primary hepatocytes were cultured for 24 hr, and the supernatants were collected and measured by the Albumin ELISA Kit (Sigma) according to the manufacturer's instructions. To measure the activity of Cyp450 enzymes, MEFs, iHeps, and primary hepatocytes were cultured in medium containing 100 μM phenacetin, 50 μM tolbutamide, 100 μM diclofenac, or 100 μM testosterone for 48 hr. Then the supernatants were collected and mixed with the same volumes of acetonitrile to stop the reaction. After centrifugation of the mixture at 12,000 × *g* for 10 min, the concentration of the metabolites in the supernatants was measured LC-MS/MS (Waters UPLC I-Class and Waters Xevo TQ-S mass spectrometer). The measured metabolites include: acetaminophen, hydroxytolbutamide, 6β-OH-testosterone, and 4′-OH-diclofenac. All compounds were also purchased from Sigma-Aldrich and used as standard samples.

Cell Transplantation

$Fah^{-/-}$ mice were supplemented with 7.5 mg/L NTBC in drinking water. According to the previous report (Sekiya and Suzuki, 2011), iHep cells (1×10^7), MEF (2×10^6), or primary hepatocyte (2×10^6) were trypsinized into single cells and suspended in 200 μL culture medium and transplanted into $Fah^{-/-}$ mice at the age of 8–12 weeks via intrasplenic injection through a left-flank incision under 1.25% tribromoethanol anesthesia. After the operation, NTBC was withdrawn from the drinking water. Blood samples from $Fah^{-/-}$ mice transplanted with MEFs were collected at day 25 (n = 3), and liver samples were collected immediately after death. The blood and liver samples of surviving mice transplanted with iHeps or primary hepatocytes were collected 8 weeks after transplantation. Total bilirubin, ALT, ALP, and AST in serum were measured.

Real-Time PCR

Total mRNA was isolated using TRIzol (Invitrogen) and 1 μg RNA was used to synthesize cDNA using the PrimeScript RT Reagent Kit (Takara Bio) according to the manufacturer's protocol. Real-time PCR was performed using the FastStart Universal Probe Master Mix (Roche) and a Stratagene Mx3000P thermal cycler. Primers sequences are supplied in Supplemental Information.

FACS Analyses

For FACS analysis, cells were trypsinized, and the single-cell suspensions were then treated with fixation/permeabilization diluent (BD Bioscience) at 4°C for 30 min, and stained with anti-albumin (Bethyl Laboratories, A90-234A), anti-ZO-1 (Gibco, 40–2200), and anti-E-cadherin (CST, 24E10) antibodies, followed by secondary antibodies conjugated with Alexa 488 (Gibco, A21428 or A11008). Wild-type MEFs or tdTomato$^+$ MEFs stained with same antibodies were uses as negative controls. Cells were then analyzed with a Guava flow cytometer (Millipore) and the data were collected with the FlowJo software.

Statistical Analyses

Values are reported as the means ± SEM. p values were calculated by Student's t test, $p < 0.05$ was considered statistically significant. All graphs were plotted with GraphPad Prism software.

SUPPLEMENTAL INFORMATION

Supplemental Information includes Supplemental Experimental Procedures and five figures and can be found with this article online at http://dx.doi.org/10.1016/j.stemcr.2017.06.013.

AUTHOR CONTRIBUTIONS

R.G. and W.T. conducted most of the experiments, analyzed the results, and wrote the paper. Q.Y. provided technical assistance with animal studies. L.H. and X.W. provided critical materials and valuable discussions. X.X. conceived the idea for the project, analyzed the results, and wrote the paper. All authors reviewed the results and approved the final version of the manuscript.

ACKNOWLEDGMENTS

This work was supported by grants from the Ministry of Science and Technology of China (2015CB964503), the Chinese Academy of Sciences (XDA01040301), the National Natural Science Foundation of China (81425024, 31371511, 81472862, and 31501189), and the Shanghai Science and Technology Committee (14ZR1409500 and 15YF1402400).

Received: February 17, 2017
Revised: June 25, 2017
Accepted: June 26, 2017
Published: July 27, 2017

REFERENCES

Bhowmick, N.A., Chytil, A., Plieth, D., Gorska, A.E., Dumont, N., Shappell, S., Washington, M.K., Neilson, E.G., and Moses, H.L. (2004). TGF-beta signaling in fibroblasts modulates the oncogenic potential of adjacent epithelia. Science *303*, 848–851.

Cerda-Esteban, N., Naumann, H., Ruzittu, S., Mah, N., Pongrac, I.M., Cozzitorto, C., Hommel, A., Andrade-Navarro, M.A., Bonifacio, E., and Spagnoli, F.M. (2017). Stepwise reprogramming of liver cells to a pancreas progenitor state by the transcriptional regulator Tgif2. Nat. Commun. *8*, 14127.

Chen, W.S., Manova, K., Weinstein, D.C., Duncan, S.A., Plump, A.S., Prezioso, V.R., Bachvarova, R.F., and Darnell, J.E., Jr. (1994). Disruption of the HNF-4 gene, expressed in visceral endoderm, leads to cell death in embryonic ectoderm and impaired gastrulation of mouse embryos. Genes Dev. *8*, 2466–2477.

Cheng, L., Hu, W., Qiu, B., Zhao, J., Yu, Y., Guan, W., Wang, M., Yang, W., and Pei, G. (2014). Generation of neural progenitor cells by chemical cocktails and hypoxia. Cell Res. *24*, 665–679.

Cicchini, C., Filippini, D., Coen, S., Marchetti, A., Cavallari, C., Laudadio, I., Spagnoli, F.M., Alonzi, T., and Tripodi, M. (2006). Snail controls differentiation of hepatocytes by repressing HNF4alpha expression. J. Cell. Physiol. *209*, 230–238.

Cirillo, L.A., Lin, F.R., Cuesta, I., Friedman, D., Jarnik, M., and Zaret, K.S. (2002). Opening of compacted chromatin by early developmental transcription factors HNF3 (FoxA) and GATA-4. Mol. Cell *9*, 279–289.

Costa, R.H., Kalinichenko, V.V., Holterman, A.X., and Wang, X. (2003). Transcription factors in liver development, differentiation, and regeneration. Hepatology *38*, 1331–1347.

Dankel, S.N., Hoang, T., Flageng, M.H., Sagen, J.V., and Mellgren, G. (2010). cAMP-mediated regulation of HNF-4alpha depends on the level of coactivator PGC-1alpha. Biochim. Biophys. Acta *1803*, 1013–1019.

Dolgikh, M.S. (2012). The clinical experience with hepatocyte transplantation for the treatment of hepatic insufficiency. Klin. Med. (Mosk) *90*, 18–22.

Du, Y., Wang, J., Jia, J., Song, N., Xiang, C., Xu, J., Hou, Z., Su, X., Liu, B., Jiang, T., et al. (2014). Human hepatocytes with drug metabolic function induced from fibroblasts by lineage reprogramming. Cell Stem Cell *14*, 394–403.

Dutkowski, P., Oberkofler, C.E., Bechir, M., Mullhaupt, B., Geier, A., Raptis, D.A., and Clavien, P.A. (2011). The model for end-stage liver disease allocation system for liver transplantation saves lives, but increases morbidity and cost: a prospective outcome analysis. Liver Transpl. *17*, 674–684.

Friedman, J.R., and Kaestner, K.H. (2006). The Foxa family of transcription factors in development and metabolism. Cell. Mol. Life Sci. *63*, 2317–2328.

Fu, Y., Huang, C., Xu, X., Gu, H., Ye, Y., Jiang, C., Qiu, Z., and Xie, X. (2015). Direct reprogramming of mouse fibroblasts into cardiomyocytes with chemical cocktails. Cell Res. *25*, 1013–1024.

Grompe, M., al-Dhalimy, M., Finegold, M., Ou, C.N., Burlingame, T., Kennaway, N.G., and Soriano, P. (1993). Loss of fumarylacetoacetate hydrolase is responsible for the neonatal hepatic dysfunction phenotype of lethal albino mice. Genes Dev. *7*, 2298–2307.

Hou, P., Li, Y., Zhang, X., Liu, C., Guan, J., Li, H., Zhao, T., Ye, J., Yang, W., Liu, K., et al. (2013). Pluripotent stem cells induced from mouse somatic cells by small-molecule compounds. Science *341*, 651–654.

Huang, P., He, Z., Ji, S., Sun, H., Xiang, D., Liu, C., Hu, Y., Wang, X., and Hui, L. (2011). Induction of functional hepatocyte-like cells from mouse fibroblasts by defined factors. Nature *475*, 386–389.

Huang, P., Zhang, L., Gao, Y., He, Z., Yao, D., Wu, Z., Cen, J., Chen, X., Liu, C., Hu, Y., et al. (2014). Direct reprogramming of human

fibroblasts to functional and expandable hepatocytes. Cell Stem Cell *14*, 370–384.

Jia, C. (2011). Advances in the regulation of liver regeneration. Expert Rev. Gastroenterol. Hepatol. *5*, 105–121.

Kaestner, K.H., Hiemisch, H., and Schutz, G. (1998). Targeted disruption of the gene encoding hepatocyte nuclear factor 3 gamma results in reduced transcription of hepatocyte-specific genes. Mol. Cell. Biol. *18*, 4245–4251.

Kasai, S., and Sawa, M. (2000). Hepatocyte transplantation for the treatment of hepatic failure. Tanpakushitsu Kakusan Koso *45*, 2301–2306.

Khetani, S.R., and Bhatia, S.N. (2008). Microscale culture of human liver cells for drug development. Nat. Biotechnol. *26*, 120–126.

Kidambi, S., Yarmush, R.S., Novik, E., Chao, P., Yarmush, M.L., and Nahmias, Y. (2009). Oxygen-mediated enhancement of primary hepatocyte metabolism, functional polarization, gene expression, and drug clearance. Proc. Natl. Acad. Sci. USA *106*, 15714–15719.

Lee, C.S., Friedman, J.R., Fulmer, J.T., and Kaestner, K.H. (2005). The initiation of liver development is dependent on Foxa transcription factors. Nature *435*, 944–947.

Levy, G., Bomze, D., Heinz, S., Ramachandran, S.D., Noerenberg, A., Cohen, M., Shibolet, O., Sklan, E., Braspenning, J., and Nahmias, Y. (2015). Long-term culture and expansion of primary human hepatocytes. Nat. Biotechnol. *33*, 1264–1271.

Li, R., Liang, J., Ni, S., Zhou, T., Qing, X., Li, H., He, W., Chen, J., Li, F., Zhuang, Q., et al. (2010). A mesenchymal-to-epithelial transition initiates and is required for the nuclear reprogramming of mouse fibroblasts. Cell Stem Cell *7*, 51–63.

Lim, K.T., Lee, S.C., Gao, Y., Kim, K.P., Song, G., An, S.Y., Adachi, K., Jang, Y.J., Kim, J., Oh, K.J., et al. (2016). Small molecules facilitate single factor-mediated hepatic reprogramming. Cell Rep. http://dx.doi.org/10.1016/j.celrep.2016.03.071.

Long, Y., Wang, M., Gu, H., and Xie, X. (2015). Bromodeoxyuridine promotes full-chemical induction of mouse pluripotent stem cells. Cell Res. *25*, 1171–1174.

Lu, H. (2016). Crosstalk of HNF4alpha with extracellular and intracellular signaling pathways in the regulation of hepatic metabolism of drugs and lipids. Acta Pharm. Sin. B *6*, 393–408.

Monaghan, A.P., Kaestner, K.H., Grau, E., and Schutz, G. (1993). Postimplantation expression patterns indicate a role for the mouse forkhead/HNF-3 alpha, beta and gamma genes in determination of the definitive endoderm, chordamesoderm and neuroectoderm. Development *119*, 567–578.

Murry, C.E., and Keller, G. (2008). Differentiation of embryonic stem cells to clinically relevant populations: lessons from embryonic development. Cell *132*, 661–680.

Niehof, M., and Borlak, J. (2009). Expression of HNF4alpha in the human and rat choroid plexus: implications for drug transport across the blood-cerebrospinal-fluid (CSF) barrier. BMC Mol. Biol. *10*, 68.

Parviz, F., Matullo, C., Garrison, W.D., Savatski, L., Adamson, J.W., Ning, G., Kaestner, K.H., Rossi, J.M., Zaret, K.S., and Duncan, S.A. (2003). Hepatocyte nuclear factor 4alpha controls the development of a hepatic epithelium and liver morphogenesis. Nat. Genet. *34*, 292–296.

Santangelo, L., Marchetti, A., Cicchini, C., Conigliaro, A., Conti, B., Mancone, C., Bonzo, J.A., Gonzalez, F.J., Alonzi, T., Amicone, L., et al. (2011). The stable repression of mesenchymal program is required for hepatocyte identity: a novel role for hepatocyte nuclear factor 4alpha. Hepatology *53*, 2063–2074.

Sasaki, H., and Hogan, B.L. (1993). Differential expression of multiple fork head related genes during gastrulation and axial pattern formation in the mouse embryo. Development *118*, 47–59.

Sekiya, S., and Suzuki, A. (2011). Direct conversion of mouse fibroblasts to hepatocyte-like cells by defined factors. Nature *475*, 390–393.

Shi, X.L., Gao, Y., Yan, Y., Ma, H., Sun, L., Huang, P., Ni, X., Zhang, L., Zhao, X., Ren, H., et al. (2016). Improved survival of porcine acute liver failure by a bioartificial liver device implanted with induced human functional hepatocytes. Cell Res. *26*, 206–216.

Shiota, G., and Yasui, T. (2012). Progress in stem cell biology in regenerative medicine for liver disease. Hepatol. Res. *42*, 15–21.

Simeonov, K.P., and Uppal, H. (2014). Direct reprogramming of human fibroblasts to hepatocyte-like cells by synthetic modified mRNAs. PLoS One *9*, e100134.

Song, G., Pacher, M., Balakrishnan, A., Yuan, Q., Tsay, H.C., Yang, D., Reetz, J., Brandes, S., Dai, Z., Putzer, B.M., et al. (2016). Direct reprogramming of hepatic myofibroblasts into hepatocytes in vivo attenuates liver fibrosis. Cell Stem Cell *18*, 797–808.

Tian, E., Sun, G., Sun, G., Chao, J., Ye, P., Warden, C., Riggs, A.D., and Shi, Y. (2016). Small-molecule-based lineage reprogramming creates functional astrocytes. Cell Rep. *16*, 781–792.

Touboul, T., Hannan, N.R., Corbineau, S., Martinez, A., Martinet, C., Branchereau, S., Mainot, S., Strick-Marchand, H., Pedersen, R., Di Santo, J., et al. (2010). Generation of functional hepatocytes from human embryonic stem cells under chemically defined conditions that recapitulate liver development. Hepatology *51*, 1754–1765.

Viollet, B., Kahn, A., and Raymondjean, M. (1997). Protein kinase A-dependent phosphorylation modulates DNA-binding activity of hepatocyte nuclear factor 4. Mol. Cell. Biol. *17*, 4208–4219.

Wang, Q., Xu, X., Li, J., Liu, J., Gu, H., Zhang, R., Chen, J., Kuang, Y., Fei, J., Jiang, C., et al. (2011). Lithium, an anti-psychotic drug, greatly enhances the generation of induced pluripotent stem cells. Cell Res. *21*, 1424–1435.

Xu, X., Wang, Q., Long, Y., Zhang, R., Wei, X., Xing, M., Gu, H., and Xie, X. (2013). Stress-mediated p38 activation promotes somatic cell reprogramming. Cell Res. *23*, 131–141.

Yu, B., He, Z.Y., You, P., Han, Q.W., Xiang, D., Chen, F., Wang, M.J., Liu, C.C., Lin, X.W., Borjigin, U., et al. (2013). Reprogramming fibroblasts into bipotential hepatic stem cells by defined factors. Cell Stem Cell *13*, 328–340.

Zhang, L., Yin, J.C., Yeh, H., Ma, N.X., Lee, G., Chen, X.A., Wang, Y., Lin, L., Chen, L., Jin, P., et al. (2015). Small molecules efficiently reprogram human astroglial cells into functional neurons. Cell Stem Cell *17*, 735–747.